Multi-Node Optical Frequency Dissemination With Post Automatic Phase Correction

Liang Hu, Xueyang Tian, Guiling Wu, *Member, IEEE*, Mengya Kong, Jianguo Shen, and Jianping Chen

***Abstract*—We report a technique for coherence transfer of laser light through a fiber link, where the optical phase noise induced by environmental perturbations via the fiber link is compensated by remote users with passive phase noise correction, rather than at the local site as is conventional. Neither phase discrimination nor active phase tracking is required due to the open-loop design, mitigating some technical problems such as the limited compensation speed and the finite compensation precision as conventional active phase noise cancellation. We theoretically analyze and experimentally demonstrate that the delay-limited residual fiber phase noise after phase noise compensation is a factor of seven higher than the conventional techniques. Using this technique, we demonstrate the transfer laser light through a 145-km-long, lab-based spooled fiber. After being compensated, a relative frequency instability is 1.9×10^{-15} at the integration time of 1 s and scales down to the level of 10^{-18}-range at 10,000 s. The frequency uncertainty of the light after transferring through the fiber relative to that of the input light is $(-0.36 \pm 2.6) \times 10^{-18}$. As the transmitted optical signal remains unaltered until it reaches the remote sites, it can be transmitted simultaneously to multiple remote sites on an arbitrarily complex fiber network, paving a way to develop a multi-node optical frequency dissemination system with post automatic phase noise correction for a number of end-users.**

***Index Terms*—Optical clock, optical fiber, passive phase cancellation, optical frequency transfer, metrology.**

I. Introduction

OPTICAL frequency references and clocks have achieved an unprecedented accuracy of better than 1 part in 10^{18}, with an instability near 1 part in 10^{19} [1]–[5]. Newly developed optical frequency dissemination schemes have attracted widespread research interest [6], [7]. Fiber-based optical frequency transfer has recognised as an ideal solution for ultra-long haul dissemination because of fiber-optic's unique advantages of broad bandwidth, low loss, and high immunity to environmental perturbations, etc [7], [8]. Thanks to the rapid development over the last decades, optical frequency dissemination with ever-increasing performance and fiber lengths are expected to play a crucial role for science and technology including time and frequency metrology [9]–[12], navigation, radio astronomy [13], [14] and tests of fundamental physics [15], [16]. To date, efforts have mainly focused on long-distance connections between just two locations connected by an optical fiber by correcting phase perturbations between the local and remote sites [8]. For example, a frequency comparision between two separated Sr optical clocks located at PTB (Germany) and SYRTE (France) has been demonstrated with a 1415-km-long optical fiber link [15] and the gravity potential difference between the middle of a mountain and a location 90 km away has been determined with a transportable Sr optical lattice clock from PTB [17].

Schemes with a variety of different topological structures that are intended to meet various application requirements, ranging from point-to-point to multi-access, cascade, and star-shaped structures, have been experimentally demonstrated. Delivering a stable optical frequency to multiple locations has been demonstrated by extracting a portion of the forward and backward transferred optical signals at any position along the fiber link as first proposed by Grosche *et al.* [18]. In this approach, many places along the fiber link can be served as an optical reference frequency and only one single fiber link stabilization control loop is necessary. A clear disadvantage of this technique is that in case of malfunction of the link stabilization system, all the access nodes will also lose access to the stabilized frequency [18]–[20]. To overcome the above main drawback, ultrastable optical frequency dissemination schemes on a star topology optical fiber network have been proposed and experimentally demonstrated [21], [22]. Using this method, the optical signal itself can be recovered at any remote sites by actively compensating the phase noise of each fiber link [21], [22].

Optical phase noise of the transmitted frequency introduced by thermal and acoustic fluctuations of the fiber link can be actively cancelled either by physically modulating the fiber length or by shifting the carrier frequency via a voltage-controlled oscillator (VCO). The main drawback related to the active phase noise correction approach is the need of complex circuits to extract the phase error and to drive the devices for phase correction in real-time e.g., frequency divider with a high ratio to avoid the cycle slips. Although the active method based on the VCOs principally has an endless compensation range, it is hard

Manuscript received December 30, 2019; revised February 14, 2020; accepted February 21, 2020. Date of publication February 24, 2020; date of current version July 20, 2020. This work was supported in part by the National Natural Science Foundation of China (NSFC) under Grant 61627871, Grant 61535006, and Grant 61905143 and in part by the Zhejiang provincial Nature Science Foundation of China under Grant LY17F050003. *(Corresponding authors: Liang Hu; Guiling Wu.)*

Liang Hu, Xueyang Tian, Guiling Wu, Mengya Kong, and Jianping Chen are with the State Key Laboratory of Advanced Optical Communication Systems and Networks, Department of Electronic Engineering, Shanghai Jiao Tong University, Shanghai 200240, China, and also with the Shanghai Institute for Advanced Communication and Data Science, Shanghai Jiao Tong University, Shanghai 200240, China (e-mail: liang.hu@sjtu.edu.cn; txy0220@sjtu.edu.cn; wuguiling@sjtu.edu.cn; kmy-mandy@sjtu.edu.cn; jpchen62@sjtu.edu.cn).

Jianguo Shen is with the College of Physics and electronic information Engineering, Zhejiang Normal University, Jinhua 321004, China (e-mail: shenjianguo981@163.com).

Color versions of one or more of the figures in this article are available online at http://ieeexplore.ieee.org.

Digital Object Identifier 10.1109/JLT.2020.2976167

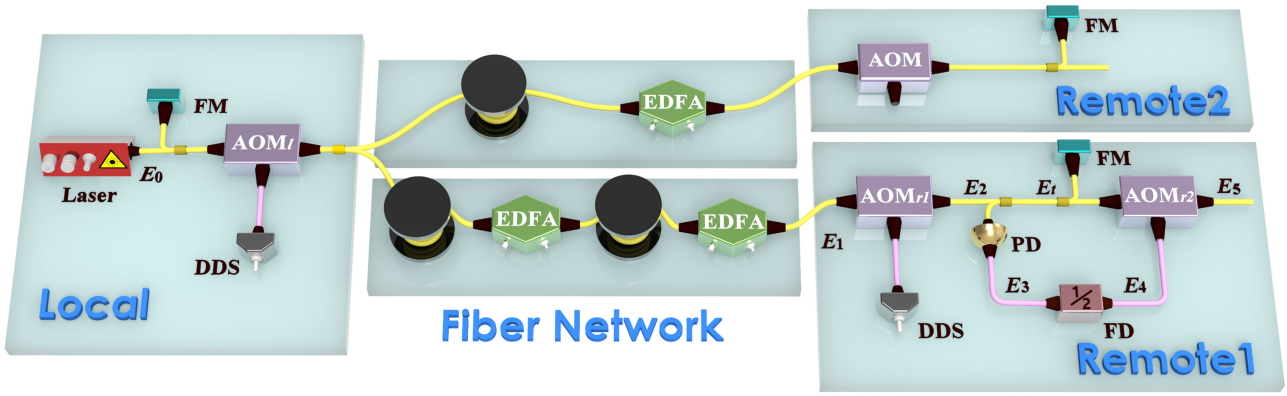

Fig. 1. Schematic diagram of our multi-node optical frequency transfer over a star topology fiber network. The optical phase noise introduced by environment perturbations on the fiber links is passively compensated at the remote sites. The yellow and pink curves indicate the optical and electrical signals, respectively. FM: Faraday mirror, DDS: direct-digital synthesizer, EDFA: erbium-doped fiber amplifier, AOM: acousto-optic modulator, PD: photo-detector, FD: frequency divider.

to achieve precise compensation because of the high voltage sensitivity of the VCOs. Additionally, the pulsing of the clock laser light and optical frequency transfer over free-space where the interruptions frequently happened call for short settling times of stabilization locks, namely the fast compensation speed, which is a great challenge even for dedicated servo amplifiers [23], [24].

The drawback of the active phase correction technique can be mitigated by using passive phase correction. Taking RF frequency transfer as an example, this novel technique is implemented by multiplying and dividing the frequency of the transferred RF frequency itself [25]–[29]. In comparison with the active technique, the passive phase correction technique would have a simple structure, a fast compensation speed, and an unlimited compensation precision. In addition, the passive phase correction technique can be achieved by both pre-phase correction in the transmitter and post-phase correction in the receiver [25], [30]. However, the passive phase noise cancellation technique used for RF frequency transfer is not directly applicable for fiber-based optical frequency dissemination by multiplying and dividing the frequency of the transferred optical carrier, such as 1550 nm, itself.

In this article, we propose a technique for coherence transfer of laser light through a star-topology fiber network, where optical phase noise induced by environmental perturbations via the fiber link is automatically compensated by remote users with passive phase noise cancellation. Theoretical analysis demonstrates the delay-limited residual fiber phase noise after phase noise compensation is a factor of 7 higher than the conventional technique. The theoretical results were compared to experimental results that were obtained for optical frequency transfer over a 145 km fiber link. The experimental results confirm that the proposed scheme with post automatic phase correction will slightly degrade the performance of the system and, however, a promising result can still be obtained.

The article is organized as follows. We illustrate the concept of multi-node optical frequency dissemination with post automatic phase noise cancellation in Section II and explain in Section III how to numerically analyze the delay limited phase noise power spectral density (PSD) based on the triple-pass scheme for the first time. In Section IV, we discuss the experimental apparatus and results. Finally, we conclude in Section V by briefly summarizing our results and providing an outlook.

II. Concept of Multi-Node Optical Frequency Dissemination

Fig. 1 shows coherence transfer of optical frequency based on a triple-pass technique with post automatic phase noise cancellation [21], [22], [31]. The laser light is coupled into a star topology fiber network. The transferred light can be extracted by each remote user. The Faraday mirrors (FMs) are separately installed at the local site and each remote site to rotate the polarization of light by 45° for making the light in the fiber link reflected multiple times. To distinguish the reflected light by the FM from the stray reflected light along the fiber network, acousto-optic modulator (AOM$_l$) and AOM$_{r1}$ with different driving frequencies are inserted at the local and remote sites, respectively. For each remote user, the driving frequency of the AOM$_{r1}$ is unique to discriminate its frequency, and an additional AOM (AOM$_{r2}$) is cascaded just after the AOM$_{r1}$ to correct the phase noise of the single-pass light. Consequently, the different frequencies of the light enable remote users at different sites to compensate for the fiber phase noise independently. The extraction and compensation of the fiber phase noise are both carried out at the remote site. This is the fundamental difference between the double-pass scheme and the triple-pass scheme as discussed in [21], [22]. The beatnote is obtained onto a photo-detector (PD) by heterodyne beating the single-pass light against the triple-pass light, acting as a phase detector that extracts the phase noise introduced by each fiber link. More importantly, using passive phase noise correction at each remote user can significantly improve the robustness of the system.

Fig. 1 shows the diagram of our multi-node optical frequency dissemination through a star topology fiber network. The electric field of the light from a narrow-linewidth laser is,

$$E_0 \propto \cos(\nu t + \phi_s), \tag{1}$$

where ν and ϕ_s are the angular frequency and the phase of the light, and here and in the following text we ignore the amplitude for conciseness. The light is passed through a local AOM (AOM_l) (downshifted mode, -1 order) working at the angular frequency of ω_l with the initial phase of ϕ_l and then coupled into a star topology fiber network. In this work, all the RF signals are provided by a direct-digital synthesizer (DDS) synchronized to a rubidium clock. At the remote site, taking the remote user 1 as an example, the fiber output light can be expressed as,

$$E_1 \propto \cos((\nu - \omega_l)t + \phi_s - \phi_l + \phi_p), \tag{2}$$

where ϕ_p is the added phase noise after transferring through the fiber. The received signal at the remote site 1 is frequency shifted by using an AOM (AOM_{r1}, upshifted mode, $+1$ order) fed by an RF signal with the angular frequency of ω_{r1} and the initial phase of ϕ_{r1}. In our configuration, we set $|\omega_{r1}| > |\omega_l|$. The electric field of the one-way is,

$$E_2 \propto \cos((\nu - \omega_l + \omega_{r1})t + \phi_s - \phi_l + \phi_p + \phi_{r1}). \tag{3}$$

Assuming that the optical phase noise introduced by environmental perturbations on the fiber link in either direction is equal, the electric field of the light after transferring through the fiber between the local site and the remote site 1 for another round-trip is,

$$E_t \propto \cos((\nu + 3(\omega_{r1} - \omega_l))t + \phi_s + 3(\phi_p + \phi_{r1} - \phi_l)). \tag{4}$$

E_t heterodyne beats against E_2 on the PD, the lower sideband of the heterodyne beatnote is,

$$E_3 \propto \cos(2(\omega_{r1} - \omega_l)t + 2(\phi_p + \phi_{r1} - \phi_l)). \tag{5}$$

Afterwards we divide the angular frequency of E_3 by a factor of 2, resulting in,

$$E_4 \propto \cos((\omega_{r1} - \omega_l)t + (\phi_p + \phi_{r1} - \phi_l)). \tag{6}$$

To compensate the phase noise introduced by the fiber link, we cascade one more AOM (AOM_{r2}) working at the downshifted mode just after the AOM_{r1}. Then we feed E_4 to the RF port of the AOM_{r2}. After being compensated, the single-way light at the remote site 1 is expressed as,

$$\begin{aligned} E_5 \propto \cos(\nu t + \phi_s) + \cos\,[(\nu + 2(\omega_{r1} - \omega_l))t \\ +\phi_s + 2(\phi_p + \phi_{r1} - \phi_l)] + \text{others}, \end{aligned} \tag{7}$$

where others represent multiple-trip optical signals between the local site and the remote site 1. We can see that the optical frequency as the first term illustrated in Eq. 7 is independent of the phase noise resulting from phase perturbations on the fiber link. The stabilized optical frequency can be filtered out by using, such as optical phase-locked loop (OPLL) techniques [32]. Additionally, the first term in Eq. 7 is independent of the RF signal with the angular frequency of ω_{r_1} at the remote site 1. In comparison with conventional approaches, this represents another advantage [21], [22].

To effectively evaluate the performance of optical frequency dissemination, we mixed the frequency-shifted optical signal E_5, which is downshifted by w_a with the initial phase of ϕ_a at the remote site 1, with the local signal E_0 onto another PD. The beating results have an expression of,

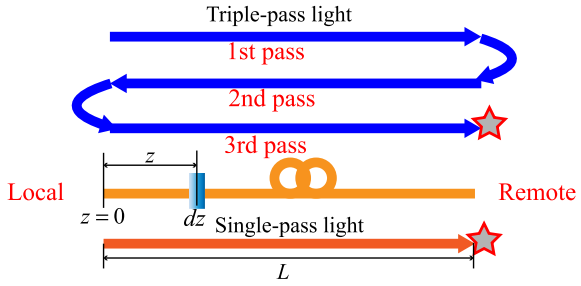

Fig. 2. Principle of optical frequency through the fiber based on the triple-pass transfer. Here L is the fiber length, and z is the distance between the local site and the remote site where the fiber phase noise occurs. The phase noise is detected at the remote site at time t by comparing the single-pass light with the triple-pass light.

$$\begin{aligned} E_6 \propto \cos(\omega_a t + \phi_a) + \cos\,[(2(\omega_{r1} - \omega_l) - \omega_a)t \\ +2(\phi_p + \phi_{r1} - \phi_l) - \phi_a] + \text{others}. \end{aligned} \tag{8}$$

With the assistance of a band-pass filter, we can effectively filter out the RF signal with the angular frequency of ω_a to evaluate the optical frequency transfer performance.

III. Delay-Limited Phase Noise PSD

In this section, we concentrate on theoretical analysis of the delay effect on fiber phase noise compensation in our proposed scheme by using the methods adopted in [20], [33]. The delay effect mainly derives from the fiber delay. As for the triple-pass scheme illustrated in Fig. 2, the light is coupled into the fiber at the local site ($z = 0$) and is transferred through the fiber for a distance of L. The fiber phase noise is collected at the remote site ($z = L$) at time $t = 0$. Thus the phase noise at the position z and at time t can be expressed as $\delta\phi(z, t)$. The fiber delay for a single pass is $\tau_0 = L/c_n$, where c_n is the speed of light in the fiber. For the single-pass light, the accumulated fiber phase noise is,

$$\phi_s(t) = \int_0^L \delta\phi[z, t - (\tau_0 - z/c_n)]dz. \tag{9}$$

The Fourier transform of the above equation is,

$$\widetilde{\phi}_s(\omega) = \int_0^L \exp(-i\omega(\tau_0 - z/c_n))\delta\widetilde{\phi}(z, \omega)dz. \tag{10}$$

Similarly, for the triple-pass light, the total fiber phase noise $\phi_t(t)$ collected by accumulating the fiber noise in the first, second and third passes has an expression of,

$$\begin{aligned} \phi_t(t) = \int_0^L \delta\phi[z, t - (3\tau_0 - z/c_n)]dz + \int_0^L \delta\phi[z, t \\ - (\tau_0 + z/c_n)]dz + \int_0^L \delta\phi[z, t - (\tau_0 - z/c_n)]dz. \end{aligned}$$

The beat signal between the single-pass light and the triple-pass light is obtained by comparing $\phi_s(t)$ with $\phi_t(t)$. It is obvious that the fiber noise of the single-pass light is equal to that from the third pass of the triple-pass light. Thus they cancel each other out, resulting in the fiber noise of the first and second passes in the beat signal. An error signal $\phi_{\text{error}}(t)$ indicating the fiber phase noise can be expressed as,

$$\phi_{\text{error}}(t) = \int_0^L [\delta\phi(z, t-(3\tau_0 - z/c_n)) + \delta\phi(z, t-(\tau_0 + z/c_n))]dz. \tag{11}$$

Assuming that the noise is uncorrelated with position, the phase-noise PSD for the fiber-induced phase noise on the one-way light is,

$$S_s(\omega) = \langle|\widetilde{\phi}_s(\omega)|^2\rangle = \int_0^L \langle|\delta\widetilde{\phi}_s(z,\omega)|^2\rangle dz. \tag{12}$$

We divided the angular frequency of the beat signal by a factor of 2 and fed the divided frequency onto the RF port of the AOM_{r2}. Thus the remaining phase noise in the optical signal can be obtained by subtracting half of the extracted phase noise ϕ_{error} from the uncompensated single-pass light,

$$\widetilde{\phi}_{\text{remote}}(\omega) = \widetilde{\phi}_s(\omega) - \frac{1}{2}\widetilde{\phi}_{\text{error}}(\omega). \tag{13}$$

With an assistance of Eq. 10 and Eq. 11, Eq. 13 becomes,

$$\widetilde{\phi}_{\text{remote}}(\omega) = \int_0^L \exp(-i\omega(\tau_0 - zc_n^{-1}))\delta\widetilde{\phi}(z,\omega)dz - \int_0^L \exp(-2i\omega\tau_0)\cos(\omega(\tau_0 - z/c_n))\delta\widetilde{\phi}(z,\omega)dz. \tag{14}$$

Again assuming spatially uncorrelated noise along the fiber, we can have $\langle|\delta\widetilde{\phi}(z,\omega)|^2\rangle = dS_s(\omega,z) = S_s(\omega)/L$. The residual phase noise PSD at the remote site is then,

$$\begin{aligned} S_{\text{remote}}(\omega) &= \left\langle \left| \int_0^L \delta\widetilde{\phi}(z,\omega)[\exp(-i\omega\tau_0)(\exp(i\omega z/c_n) - \exp(-i\omega\tau_0)\cos(\omega(\tau_0 - z/c_n)))]dz \right|^2 \right\rangle \\ &\simeq \left(\frac{3}{2} - \cos(2\omega\tau_0) - \frac{1}{2}\text{sinc}(2\omega\tau_0)\right) S_s(\omega), \end{aligned}$$

Trigonometric functions can be expanded with the Taylor expansion when $\omega\tau_0 \ll 1$, so $\cos(x) \simeq 1 - x^2/2 + \mathcal{O}(x)^4$ and $\text{sinc}(x) \simeq 1 - x^2/6 + \mathcal{O}(x)^4$. By inserting the expansion results into the above equation, then the residual phase noise PSD at the remote site yields,

$$S_{\text{remote}}(\omega) \simeq \left(\frac{7}{3}(\omega\tau_0)^2 + \mathcal{O}(\omega\tau_0)^4\right) S_s(\omega). \tag{15}$$

Once we ignore the high order term of $\mathcal{O}(\omega\tau_0)^4$, the phase noise PSD has an expression of,

$$S_{\text{remote}}(\omega) \simeq \frac{7}{3}(\omega\tau_0)^2 S_s(\omega). \tag{16}$$

The result indicates that the fiber phase noise cannot be thoroughly compensated because of the delay effect. In comparison with the conventional double-pass technique, the phase noise rejection capability of both the conventional and proposed techniques is proportional to τ_0^2 and the uncompensated single-pass fiber phase noise PSD, $S_s(\omega)$. However, the residual fiber phase noise PSD in the proposed technique turns out to be a factor of 7 worse than that of in the conventional double-pass scheme [20], [33].

IV. Experimental Apparatus and Results

A. Experimental Apparatus

We have demonstrated this technique by using the simplest configuration that possesses all the critical elements for optical frequency transfer over a star topology fiber network. The proposed scheme was tested by using a narrow-linewidth optical source (NKT X15) at a frequency near 193 THz with a linewidth of 100 Hz. To simulate a start topology network, the signal source was then split equally into two parts, one part being transmitted along a 145 km spooled fiber link to the remote site 1. Due to the limited available components, here we only test the remote site 1. Two home-made bidirectional erbium-doped fiber amplifiers (EDFAs) have been adopted after 70 km and 145 km fiber link for boosting the fading optical signal. This proof-of-principle demonstration was over 145 km, but the technique is equally applicable to a longer fiber link inserting more bidirectional amplifiers along the fiber link [11], [12]. To avoid nonlinear effects, the signal power launched into the fiber link is kept low (6 mW in our case). At the same time, the signal power arriving at the PD is maintained at 1 mW or below. The angular frequencies of AOMs at the local and remote sites are $\omega_l = 2\pi \times 45$ MHz (AOM_l, downshifted mode, -1 order), $\omega_{r1} = 2\pi \times 80$ MHz (AOM_{r1}, upshifted mode, $+1$ order), respectively. Here before feeding E_4 with the angular frequency of $\omega_{r1} - \omega_l$ onto the RF port of the AOM_{r2} (downshifted mode, -1 order) to compensate the phase noise of the single-pass light, we mixed E_4 with ω_a and extracted the upper sideband with the frequency of 80 MHz for the AOM_{r2}. With this configuration, we can acquire an out-of-loop heterodyne beat frequency of 45 MHz.

To measure the phase noise of the stabilized optical frequency at the remote site 1, we perform the measurement by feeding the heterodyne beat frequency together with a stable RF frequency signal from the DDS to a phase detector. The voltage fluctuations at the phase detector output are then measured with an fast Fourier transform (FFT) analyzer to obtain the phase fluctuations $S_\phi(\omega)$. Here we measured the phase noise PSD for the stabilized fiber link and for the free-running link where no noise cancellation was applied. Additionally, to effectively measure the transfer stability to the remote site 1, we use a frequency counter, which is referenced to the DDS at the local site, to record the out-of-loop heterodyne beat frequency.

B. Back-to-Back System

We measured the noise floor by optically short-cutting the stabilized link by connecting the output of the local AOM_l

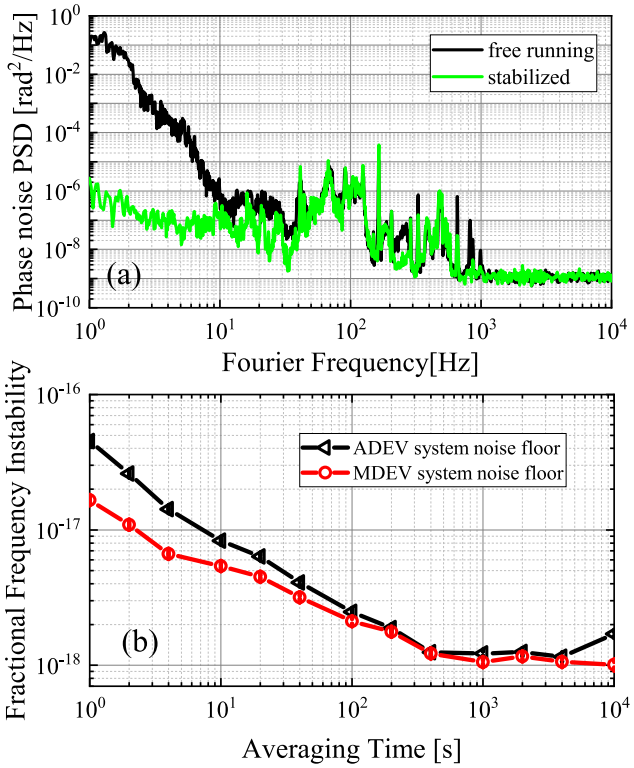

Fig. 3. System noise floor measurement results. (a) Measured phase noise PSD of the free-running back-to-back system (black curves) and stabilized back-to-back system (green curves). (b) Black left triangles and red circles are, respectively, measured fractional frequency instabilities of the stabilized back-to-back system derived from a nonaveraging (Π-type) frequency counter in terms of ADEV and an averaging (Λ-type) frequency counter in terms of MDEV. The error bars are inside the symbols.

to the input of the remote AOM using an optical attenuator. Fig. 3(a) shows that a widespread frequency domain characterization of the phase instability is the PSD of phase fluctuations $S_\phi(f) = \langle|\tilde{\phi}(\omega)|^2\rangle$ for the out-of-loop beat signal of the unstabilized and stabilized back-to-back system, respectively. The phase noise of the unstabilized back-to-back system (black curve in Fig. 3(a)) is dominated by $S_\phi(f) \sim 10^{-1}/f^5$ rad^2/Hz up to a Fourier frequency of $f = 10$ Hz and by a white phase noise of $S_\phi(f) = h_2/f^0$ rad^2/Hz ($h_2 \simeq 10^{-9}$) above 10 Hz. There are some bumps appeared between 10 Hz and 1 kHz and we currently could not identify the source of these bumps. Once the back-to-back system is stabilized by means of the proposed passive phase noise cancellation technique, the fluctuations of the path length and those arising from devices that are inside the loop are corrected. The phase noise is suppressed by approximately 50 dB at 1 Hz. The stabilized back-to-back system is dominated by a white phase noise level of $S_\phi(f) \sim 10^{-7}/f^0$ rad^2/Hz. Fig. 3(b) illustrates the corresponding fractional frequency instability. Measurements of the frequency instability for longer averaging times calculated by overlapping Allan deviation (ADEV) (triangles) and modified Allan deviation (MDEV) (circles) taken with the counters operating in Π-averaging type and Λ-averaging type, respectively, with a 1 s gate time [34]. We can clearly see that the variable noise floor, which for the averaging time beyond around 300 s is approximately 10^{-18}.

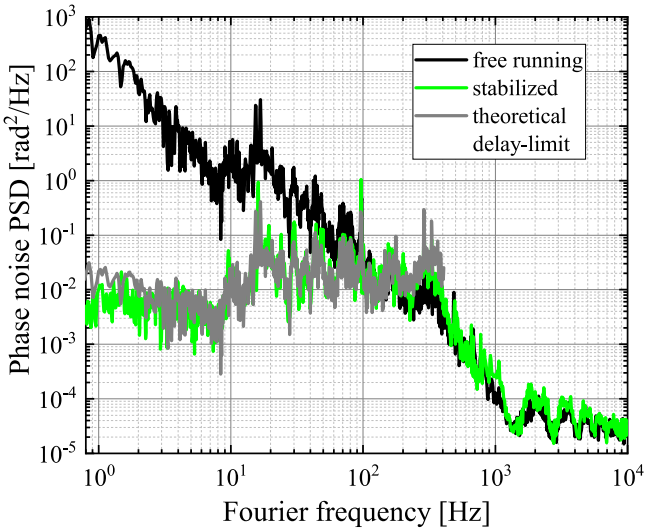

Fig. 4. Measured phase noise PSD of the 145 km free-running (black curve) and stabilized link with passive phase noise cancellation (green curve). The gray curve is the theoretical prediction by using Eq. 16.

We attribute the variation in the 10^{-18} range to the temperature fluctuations of the optical paths outside the loop [33]. Therefore, we regard the observed instability around 10^{-18} as fortuitous in our present setup, where the temperature of the optical setups is not controlled passively or actively. To further determine the electronic noise limit of our measurement capabilities, the electrical path was locked to an RF synthesizer and its frequency was counted. A fractional frequency instability in terms of the ADEV $1.6 \times 10^{-17}/\tau$ was achieved which includes electronic noise due to the RF components and the frequency counting system.

C. *Optical Frequency Transfer Over a Fiber Limk*

Fig. 4 shows the phase noise PSD for the 145 km stabilized fiber link (green curve), and for the 145 km free-running link (black curve), where no phase noise cancellation was applied. We find that unlocked phase noise on our fiber link approximately follows a power-law dependence, $S_\phi(f) \sim h_0/f^2$ rad^2/Hz, for $f < 1$ kHz, indicating that the white frequency noise is dominating in the free-running fiber link, where $h_0 \sim 430$ is the white frequency noise coefficient that varies with different fiber links. Once the fiber noise cancellation system at the remote site 1 is applied, the phase noise PSD is remarkably suppressed down to $\sim 10^{-2}$ rad^2/Hz within its delay-unsuppressed below $1/4\tau_0 \simeq 345$ Hz, showing the remaining noise is mainly determined by the white phase noise. It is important to note that strong servo bumps disappeared. In comparison with conventional active phase noise cancellation schemes, the disappeared servo bumps represent another advantage because this reduces the integrated phase noise [33]. From Fig. 4, we also can find the measured locked phase noise to be in good agreement with the theoretical value (gray curves) as predicted in Eq. 16. This, on the other hand, confirms the correctness of the theoretical model presented in Section III.

Complementary to the frequency-domain characterization, a time-domain feature of the fractional frequency instability is

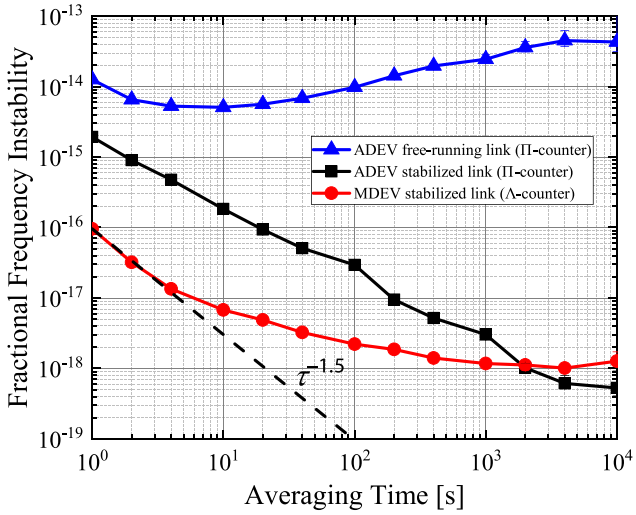

Fig. 5. Measured fractional frequency instability of the 145-km free-running fiber link (blue up triangles) and the stabilized link (black squares) derived from a nonaveraging (Π-type) frequency counter and expressed as the ADEV. To obtain a significantly shorter measurement time and to distinguish between white phase, flicker phase, and other noise types, an averaging (overlapping Λ-type) frequency counter is used for which the MDEV (red circles) measures the instability. The dashed curve shows the MDEV of $9.6 \times 10^{-17}/\tau^{\frac{3}{2}}$. The error bars are inside the symbols.

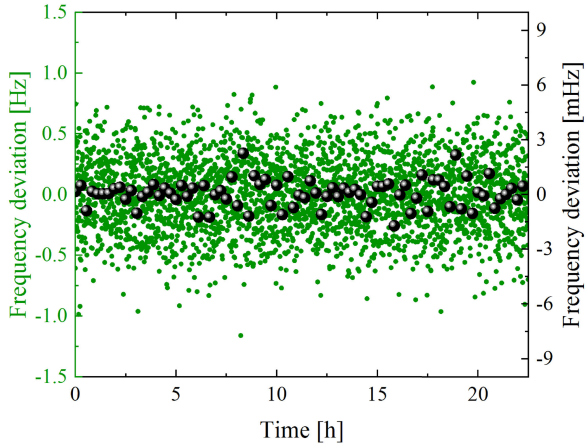

Fig. 6. Frequency deviation of the transferred light from the expected value when transferring through the 145-km fiber link (green dots, left frequency axis). The relative frequency deviation is measured by a Π-type frequency counter. The arithmetic means of all cycle-slip free 1,000 s intervals have been computed. From the resulting 81 data points (black dots, right frequency axis), a fractional difference between sent and transferred frequency of $(-0.36 \pm 2.6) \times 10^{-18}$ is calculated.

performed. Fig. 5 shows the instability of the free-running link (up triangles). It fluctuates in the 10^{-14} range with an overall mean of the fractional frequency instability of here $\sim 2 \times 10^{-14}$. The instability indicates processes with several periods of temperature fluctuations. In the case of the stabilized link in terms of the ADEV, it is around 1.9×10^{-15} at the averaging time of 1 s and reaches a floor in the 10^{-18}-range for a few thousand of seconds of averaging time. The filled circles represent the result of applying the MDEV formula to the Λ-type data. The Λ-MDEVs fall off as $9.6 \times 10^{-17}/\tau^{\frac{3}{2}}$ for averaging times up to a few seconds as expected e.g. for white phase noise. For the measurement, a flicker frequency noise floor around 10^{-18} seems to be reached after about 1,000 s of averaging time τ. This is to be expected from the variations of the current noise floor of the setup without the long fiber link as shown in Fig. 3(b). It is important to stress that the slight difference in long-term stability between the MDEV and ADEV is mainly due to the different temperature conditions at different test times.

Fig. 6 displays the frequency deviation of the transferred light from the expected value. Here we recorded the relevant beatnotes with a 1 s gate time and with a Π-type counter to avoid overweighting the center parts of the data sets with the triangular weighting of the Λ-type counter. The frequency of the beat signal was measured in 81,000 s. The distribution of the frequency deviation over counts follows a Gaussian function. We divided the data set into 81 subsets with a length of continuous 1,000 s time period. The mean value of each subset is calculated, as shown with black filled circles in Fig. 6. The 81 data points have an arithmetic mean of -68.7 μHz (-3.6×10^{-19}) and a standard deviation of 494 μHz (2.6×10^{-18}). Consequently, the statistical fractional uncertainty of the 81,000 data points is calculated to be $(-0.36 \pm 2.6) \times 10^{-18}$.

Note that in the current setup we only stabilize the fiber path starting at the input of the AOM at the local site and ending at the FM at the remote site 1, but thermal and acoustic perturbations affecting all other fibers or fiber components involved in the optical carrier transfer path. In particular, the back-to-back system was built with a fiber-pigtailed AOM (AOM_{r2}), which caused non-optimal spatial design and thus involved relatively long uncompensated fibers and thermal effect. Although the accuracy currently achieved in the laboratory spool fiber that is quieter than the filed-deployed fiber is not enough to meet the requirements of remote comparisons of optical atomic clocks [15], [17], [35], we believe that the system performance could be improved by actively and passively stabilizing the temperature of the back-to-back system [11], [36], [37] or by building the system with free-space optics as performed in [33].

Because of the similarity among the test results of different remote sites, we just show the test results of a typical remote site in a star topology fiber network. As discussed in [21], [22], our scheme, in principle, can support multiple users simultaneously by choosing different AOM-driving frequencies in different channels to make the beatnotes at different remote users shift by a few megahertz. Then in each channel, the remote user uses a narrow bandwidth band-pass filter to filter out the signal for noise compensation. The number of remote users for this scheme will be determined by some technical problems such as the bandwidth of the band-pass filters. Additionally, there is 3 dB insertion loss by adding one more remote site, proper EDFAs and electrical amplifiers can be used to amplify the desired optical signals and detected RF signals. Thus, it ensures that multiple remote sites can be inserted in a star topology fiber network.

V. Conclusion

In summary, we have presented a new method, making a stable optical frequency available at remote user sites. The phase drift generated by fiber-length variations can be automatically

eliminated by optical frequency mixing and shifting at the remote sites with the assistance of AOMs. Neither phase discrimination nor active phase tracking is required due to the open-loop design, mitigating some technical difficulties in conventional active phase noise cancellation. Moreover, our approach, in principle, is independent of the remote RF signal source. Consequently, the RF signal source with a high frequency stability is no longer needed, which simplifies the system and makes the system cost-effective. We experimentally demonstrated the transfer of optical frequency to one remote site through a 145 km, lab-based spooled fiber link. After being compensated, optical frequency transfer with the relative frequency instability of 1.9×10^{-15} at 1 s and reaches a floor in the 10^{-18}-range after a few thousand of seconds was obtained. The frequency uncertainty of the light after transferring through the fiber relative to that of the input light is $(-0.36 \pm 2.6) \times 10^{-18}$ for the 145 km fiber link.

The proposed technique considerably simplifies future efforts to make coherent optical frequency signals available to many users, enabling the above mentioned applications, and paving a path towards a redefinition of the unit of time, the SI second through regular and practical international comparisons of optical clocks [35], [38]–[41].

REFERENCES

[1] A. D. Ludlow, M. M. Boyd, J. Ye, E. Peik, and P. O. Schmidt, "Optical atomic clocks," *Rev. Mod. Phys*, vol. 87, no. 2, 2015, Art. no. 637.

[2] N. Poli, C. Oates, P. Gill, and G. Tino, "Optical atomic clocks," *Riv. Nuovo Cimento*, vol. 36, 2013, Art. no. 555.

[3] G. E. Marti, R. B. Hutson, A. Goban, S. L. Campbell, N. Poli, and J. Ye, "Imaging optical frequencies with 100 μHz precision and 1.1 μm resolution," *Phys. Rev. Lett.*, vol. 120, 2018 Art. no. 103201.

[4] M. Schioppo *et al.*, "Ultrastable optical clock with two cold-atom ensembles," *Nat. Photon.*, vol. 11, pp. 48–52, 2016.

[5] W. F. McGrew *et al.*, "Atomic clock performance enabling geodesy below the centimetre level," *Nature*, vol. 564, no. 7734, pp. 87–90, 2018.

[6] F. R. Giorgetta, W. C. Swann, L. C. Sinclair, E. Baumann, I. Coddington, and N. R. Newbury, "Optical two-way time and frequency transfer over free space," *Nat. Photon.*, vol. 7, pp. 434–438, 2013.

[7] F. Riehle, "Optical clock networks," *Nat. Photon.*, vol. 11, pp. 25–31, Jan. 2017.

[8] L.-S. Ma, P. Jungner, J. Ye, and J. L. Hall, "Delivering the same optical frequency at two places: Accurate cancellation of phase noise introduced by an optical fiber or other time-varying path," *Opt. Lett.*, vol. 19, no. 21, pp. 1777–1779, 1994.

[9] S. M. Foreman, A. D. Ludlow, M. H. De Miranda, J. E. Stalnaker, S. A. Diddams, and J. Ye, "Coherent optical phase transfer over a 32-km fiber with 1 s instability at 10^{-17}," *Phys. Rev. Lett.*, vol. 99, no. 15, 2007, Art. no. 153601.

[10] C. Daussy *et al.*, "Long-distance frequency dissemination with a resolution of 10^{-17}," *Phys. Rev. Lett.*, vol. 94, no. 20, 2005, Art. no. 203904.

[11] S. Droste *et al.*, "Optical-frequency transfer over a single-span 1840 km fiber link," *Phys. Rev. Lett.*, vol. 111, no. 11, 2013, Art. no. 110801.

[12] D. Calonico *et al.*, "High-accuracy coherent optical frequency transfer over a doubled 642-km fiber link," *Appl. Phys. B*, vol. 117, no. 3, pp. 979–986, 2014.

[13] C. Clivati *et al.*, "A VLBI experiment using a remote atomic clock via a coherent fibre link," *Sci. Rep.*, vol. 7, 2017, Art. no. 40992.

[14] B. Wang, X. Zhu, C. Gao, Y. Bai, J. Dong, and L. Wang, "Square kilometre array telescope—precision reference frequency synchronisation via 1f-2f dissemination," *Sci. Rep.*, vol. 5, 2015, Art. no. 13851.

[15] C. Lisdat *et al.*, "A clock network for geodesy and fundamental science," *Nat. Commun.*, vol. 7, 2016, Art. no. 12443.

[16] L. Hu, N. Poli, L. Salvi, and G. M. Tino, "Atom interferometry with the Sr optical clock transition," *Phys. Rev. Lett.*, vol. 119, no. 26, 2017, Art. no. 263601.

[17] J. Grotti *et al.*, "Geodesy and metrology with a transportable optical clock," *Nature Phys.*, vol. 14, pp. 437–441, 2018.

[18] G. Grosche, "Eavesdropping time and frequency: phase noise cancellation along a time-varying path, such as an optical fiber," *Opt. Lett.*, vol. 39, no. 9, pp. 2545–2548, 2014.

[19] Y. Bai, B. Wang, X. Zhu, C. Gao, J. Miao, and L. Wang, "Fiber-based multiple-access optical frequency dissemination," *Opt. Lett.*, vol. 38, no. 17, pp. 3333–3335, 2013.

[20] A. Bercy *et al.*, "In-line extraction of an ultrastable frequency signal over an optical fiber link," *J. Opt. Soc. America B*, vol. 31, no. 4, pp. 678–685, 2014.

[21] S. W. Schediwy *et al.*, "High-precision optical-frequency dissemination on branching optical-fiber networks," *Opt. Lett.*, vol. 38, no. 15, pp. 2893–2896, 2013.

[22] L. Wu, Y. Jiang, C. Ma, H. Yu, Z. Bi, and L. Ma, "Coherence transfer of subhertz-linewidth laser light via an optical fiber noise compensated by remote users," *Opt. Lett.*, vol. 41, no. 18, pp. 4368–4371, 2016.

[23] S. Falke, M. Misera, U. Sterr, and C. Lisdat, "Delivering pulsed and phase stable light to atoms of an optical clock," *Appl. Phys. B*, vol. 107, no. 2, pp. 301–311, 2012.

[24] D. Gozzard, S. Schediwy, B. Stone, M. Messineo, and M. Tobar, "Stabilized free-space optical frequency transfer," *Phys. Rev. Appl.*, vol. 10, no. 2, 2018, Art. no. 024046.

[25] S. Pan, J. Wei, and F. Zhang, "Passive phase correction for stable radio frequency transfer via optical fiber," *Photon. Netw. Commun.*, vol. 31, no. 2, pp. 327–335, 2016.

[26] Y. He *et al.*, "Stable radio-frequency transfer over optical fiber by phase-conjugate frequency mixing," *Opt. Express*, vol. 21, no. 16, pp. 18 754–18 764, 2013.

[27] R. Huang, G. Wu, H. Li, and J. Chen, "Fiber-optic radio frequency transfer based on passive phase noise compensation with frequency dividing and filtering," *Opt. Lett.*, vol. 41, no. 3, pp. 626–629, 2016.

[28] D. Li, D. Hou, E. Hu, and J. Zhao, "Phase conjugation frequency dissemination based on harmonics of optical comb at 10- 17 instability level," *Opt. Lett.*, vol. 39, no. 17, pp. 5058–5061, 2014.

[29] L. Yu *et al.*, "Stable radio frequency dissemination by simple hybrid frequency modulation scheme," *Opt. Lett.*, vol. 39, no. 18, pp. 5255–5258, 2014.

[30] Z. Wu, Y. Dai, F. Yin, K. Xu, J. Li, and J. Lin, "Stable radio frequency phase delivery by rapid and endless post error cancellation," *Opt. Lett.*, vol. 38, no. 7, pp. 1098–1100, 2013.

[31] C. Ma, L. Wu, J. Gu, Y. Chen, and G. Chen, "Delay effect on coherent transfer of optical frequency based on a triple-pass scheme," *Chin. Phys. Lett.*, vol. 35, no. 8, 2018, Art. no. 080601.

[32] V. Ferrero and S. Camatel, "Optical phase locking techniques: an overview and a novel method based on single side sub-carrier modulation," *Opt. Express*, vol. 16, no. 2, pp. 818–828, 2008.

[33] P. A. Williams, W. C. Swann, and N. R. Newbury, "High-stability transfer of an optical frequency over long fiber-optic links," *J. Opt. Soc. America B*, vol. 25, no. 8, pp. 1284–1293, 2008.

[34] S. T. Dawkins, J. J. McFerran, and A. N. Luiten, "Considerations on the measurement of the stability of oscillators with frequency counters," *IEEE Trans. Ultrason. Ferroelectr. Freq. Control*, vol. 54, no. 5, pp. 918–925, May 2007.

[35] W. F. McGrew *et al.*, "Towards the optical second: verifying optical clocks at the SI limit," *Optica*, vol. 6, no. 4, pp. 448–454, 2019.

[36] K. Predehl *et al.*, "A 920-kilometer optical fiber link for frequency metrology at the 19th decimal place," *Science*, vol. 336, no. 6080, pp. 441–444, 2012.

[37] S. Droste *et al.*, "Optical frequency transfer via 1840 km fiber link with superior stability," in *Proc. CLEO: Sci. Innov.*, 2014, pp. SW3O–3.

[38] E. Oelker *et al.*, "Demonstration of 4.8×10^{-17} stability at 1 s for two independent optical clocks," *Nat. Photon.*, vol. 13, no. 10, pp. 714–719, 2019.

[39] H. Hachisu, F. Nakagawa, Y. Hanado, and T. Ido, "Months-long real-time generation of a time scale based on an optical clock," *Sci. Rep.*, vol. 8, no. 1, 2018, Art. no. 4243.

[40] J. Yao, T. E. Parker, N. Ashby, and J. Levine, "Incorporating an optical clock into a time scale," *IEEE Trans. Ultrason. Ferroelectr. Freq. Control*, vol. 65, no. 1, pp. 127–134, 2017.

[41] C. Grebing *et al.*, "Realization of a timescale with an accurate optical lattice clock," *Optical*, vol. 3, no. 6, pp. 563–569, 2016.

Liang Hu received the B.S. degree from Hangzhou Dianzi University, Hangzhou, China, in 2011, and the M.S. degree from Shanghai Jiao Tong University, Shanghai, China, in 2014. He received the Ph.D. degree from the University of Florence, Florence, Italy, in 2017 during which he was a Marie-Curie Early Stage Researcher at FACT project. He is currently a Tenure-Track Assistant Professor with the State Key Laboratory of Advanced Optical Communication Systems and Networks, Department of Electronic Engineering, Shanghai Jiao Tong University. His current research interests include photonic signal transmission and atom interferometry.

Xueyang Tian received the B.S. degree from Shanghai Dianji University, Hangzhou, China, in 2017. She is currently working toward the graduate degree with the State Key Laboratory of Advanced Optical Communication Systems and Networks, Department of Electronic Engineering, Shanghai Jiao Tong University, Shanghai, China. Her current research interests include photonic signal transmission.

Guiling Wu (Member, IEEE) received the B.S. degree from the Ha Er Bing Institute of Technology, China, in 1995, and the M.S. and Ph.D. degrees from the Huazhong University of Science and Technology, Huazhong, China, in 1998 and 2001, respectively. He is currently a Professor with the State Key Laboratory of Advanced Optical Communication Systems and Networks, Department of Electronic Engineering, Shanghai Jiao Tong University, China. His current research interests include photonic signal processing and transmission.

Mengya Kong received the B.S degree from the Nanjing University of Posts and Telecommunications, Nanjing, China, in 2017. She is currently working toward the graduate degree with the State Key Laboratory of Advanced Optical Communication Systems and Networks, Department of Electronic Engineering, Shanghai Jiao Tong University, Shanghai, China. Her research interests include opto-electronic devices and RF circuit integration, microwave frequency transfer, and system applications.

Jianguo Shen received the bachelor‘s degree in physics educations from Zhengjiang Normal University, Jinhua, China, in 2002, the master’s degree in circuit and system from Hangzhou Dianzi University, Hangzhou, China, in 2007, and the Ph.D. degree in electromagnetic and microwave technology from Shanghai Jiaotong University, Shanghai, China, in 2015. He is currently an Associate Professor with Zhejiang Normal University of China, Jinhua. His research interests include microwave photonic signals processing and time and frequency transfer over the optical fiber.

Jianping Chen received the B.S. degree from Zhejiang University, Hangzhou, China, in 1983, and the M.S. and Ph.D. degrees from Shanghai Jiao Tong University, Shanghai, China, in 1986 and 1992, respectively. He is currently a Professor with the State Key Laboratory of Advanced Optical Communication Systems and Networks, Department of Electronic Engineering, Shanghai Jiao Tong University. His main research interests include opto-electronic devices and integration, photonic signal processing, and system applications. He is a Principal Scientist of National Basic Research Program of China (also known as 973 Program).